

Gust Response Evaluation of Cable-Stayed Bridges under Erection using Gust Response Analysis and Elastic Model

Y. Ito¹⁾, Y. Nakashima²⁾, H. Kobayashi³⁾ and Y. Sakai¹⁾

¹Institute of Technology, Shimizu Corporation, Tokyo, 135-8530, Japan

²Hokkaido Branch, Shimizu Corporation, Hokkaido, 068-2111, Japan

³International Division, Shimizu Corporation, Ho Chi Minh City, Vietnam

Abstract

Gust response is one of the most important wind-induced oscillations in the design of long-span bridges. Large-amplitude vertical oscillations can be generated, especially in the erection stage. Elastic model tests and gust response analysis are usually conducted to estimate the amplitude. However, the experimental cost for an elastic model test is much higher than that for section model tests, while the accuracy of gust response analysis has not been investigated well yet. This study is carried out to investigate the accuracy of vertical gust response analysis of a cable-stayed bridge under erection by comparing analysis results with elastic model results. It was clarified that gust response analysis at the erection stage is a reliable means of evaluation when appropriate wind force coefficients are used.

Introduction

Wind-resistant design is one of the most important procedures in the design of long-span bridges. In addition to studying the wind forces acting on bridges, the stability of bridges against wind-induced vibration, such as vortex-induced vibration, flutter, and gust response should also be investigated. The stability against wind at the erection stage is usually lower than that at the completion stage even though the expected wind speed during erection is lower than the design wind speed. Gust response can be the most critical wind-induced phenomenon during the erection of a bridge, and its amplitude can be investigated only by elastic model tests or gust response analysis, while vortex-induced vibration and flutter can be investigated by wind tunnel tests using a section model. Gust response analysis has an advantage over the elastic model tests in terms of cost and time. On the other hand, elastic model tests have an advantage in terms of accuracy since the accuracy of gust response analysis is investigated only in few studies [4]. The results of gust response analyses have discrepancies with experimental results under some conditions even in simplified cases [4].

This study is carried out to clarify the accuracy of gust response analysis by comparing analysis results with elastic model test results. The wind force coefficients used in gust response analysis are measured in this study using a section model. A free vibration test using an elastic model is conducted to obtain validation data. Gust response analyses are conducted using measured wind force coefficients, and the results are compared with the elastic model test results.

Experimental Conditions

Model Bridge

A pre-stressed concrete cable-stayed bridge is used in this study as a model bridge. The girder has two box shapes with a 3.0 m height and 30.0 m width, as shown in Figure 1. The main span

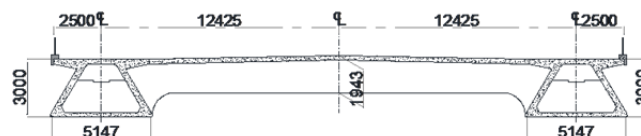


Figure 1. Girder shape of the model bridge

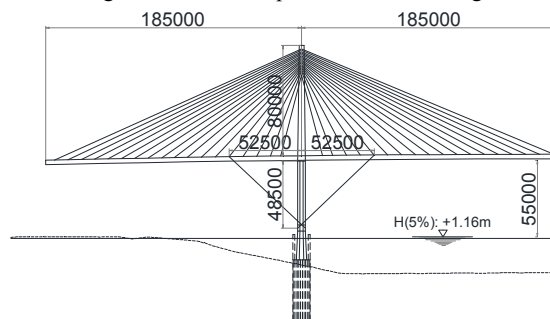


Figure 2. Structural arrangement of the model bridge

Mode	Natural Freq.	Equivalent Mass
1 st Vertical	0.065 Hz	54.1 t/m
1 st Horizontal	0.080 Hz	46.9 t/m
1 st Torsional	0.356 Hz	5251.1 tm ² /m

Table 1. Natural frequencies and equivalent masses of the model bridge

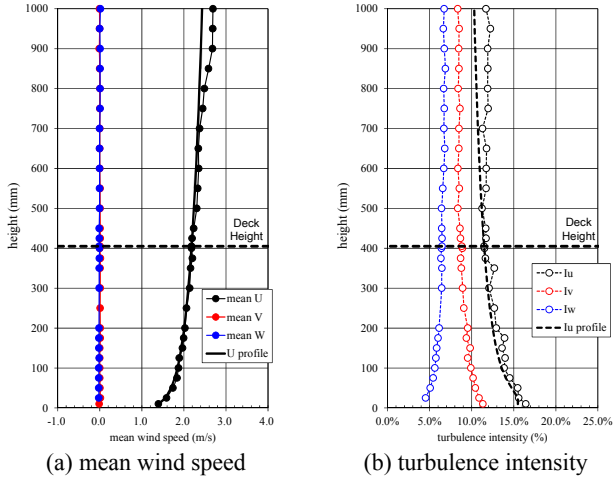
length of this model bridge is set as 375 m, and the maximum overhanging length at the erection stage is 185 m as shown in Figure 2. Temporary cables were installed from pier to girders during the erection stage to increase the rigidity. The natural frequencies and equivalent masses of the 1st vertical, horizontal, and torsional modes at the stage shown in Figure 2 are listed in Table 1. The natural frequency of the 1st vertical mode is quite small since this bridge has no intermediate piers in the side span. The design wind speed is set as 27 m/s. The roughness parameter per Japanese wind-resistant design standards is set as Category I. The power law index of this category is 0.12.

Section Model Tests

Section model wind tunnel tests are carried out to measure lift coefficients and flutter derivatives in smooth and turbulent flows. These tests are carried out in an Eiffel-type wind tunnel with a test section of 0.9 m height and 1.1 m width. The scale of the model is 1/100, and the length of the model is 1.0 m. The flow characteristics of the wind tunnel were measured in the smooth and turbulent flows before wind force measurements. The turbulence intensity of the smooth flow is less than 1.0%. The turbulent flow is generated by a turbulence grid with 60 mm width, 31 mm depth, and 290 mm intervals. The turbulence intensity is approximately 11%, and the turbulence scale is



Figure 3. Set up for section model tests



(a) mean wind speed (b) turbulence intensity
Figure 4. Vertical profiles of mean wind speeds and turbulence intensities

approximately 10 m in the stream-wise direction and 3.5 m in the vertical direction in the real scale.

The static wind force acting on the model is measured by changing the angle of attack from -15° to $+15^\circ$ at intervals of 1° . Two mean wind speeds are used to check the effect of the Reynolds number on the static wind force coefficients. The model is supported by two sets of three-component force strain gage balance devices (Nissho Electric Works Co. Ltd., Multi Component Load Cell LMC-3501-50N); these devices are fixed on the angle controller (Shimizu Corporation, DW289). The outputs from these devices are measured using an AD converter (Graphtec, Data Platform GL7000 and GL7-V) with a sampling frequency of 1.0 kHz and a data number of 65,536 through DC amplifiers (Nissho Electric Works Co. Ltd., DSA-100) with 224 Hz low-pass filters (JEIC, low-pass filter type 3102).

The aerodynamic force acting on the model is measured using the forced vibration method. A harmonic oscillation in the vertical direction or torsional direction is provided to the model using actuating devices, and the unsteady wind forces acting on the model are measured. The basic set-up of the test is the same as that of the static wind force measurement test. Laser displacement sensors (Keyence, IL-300) are installed to measure displacements of the model. The oscillation frequency is approximately 2.0 Hz, and half amplitudes of the oscillation are 10 mm in the vertical direction and 2.29° in the torsional direction.

Elastic Model Tests

Free vibration tests are carried out using the elastic model with a 1/150 scale in turbulent flow. This test is carried out in a Göttingen type wind tunnel at Shimizu Corporation. The test section is 3.5 m in width and 2.5 m in height. Appropriate boundary layer turbulence is generated before conducting free vibration tests in the wind tunnel. Vertical profiles of the mean wind speeds and turbulence intensities are shown in Figure 4, and

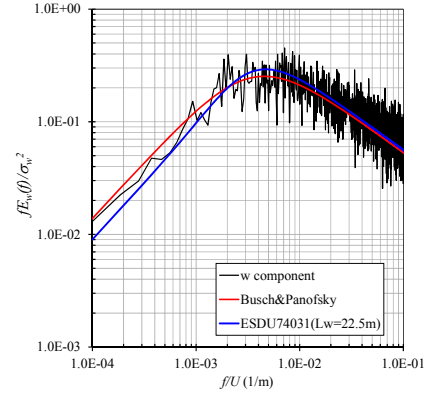


Figure 5. Power spectrum of vertical component of fluctuating wind (in real-scale)

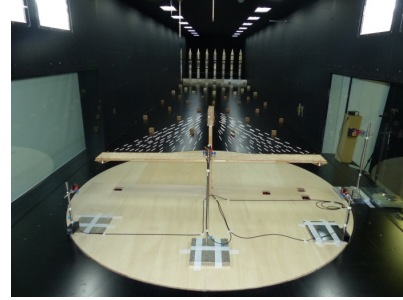


Figure 6. Experimental set up for elastic model tests

they are in good agreement with the target profiles prescribed by Japanese wind-resistant design standards. The turbulence intensity of the vertical component is 6.5% at the deck height. The power spectrum of the vertical component of fluctuating wind is shown in Figure 5. The Busch & Panofsky spectrum [1] used in the gust response analysis and the Karman-type spectrum [2] are plotted in the same figure. The power spectrum is in good agreement with both spectrums, and the generated turbulence has appropriate mean wind speed, turbulence intensity profiles, and turbulence scale.

The target modes of the elastic model tests are the 1st vertical and 1st horizontal modes. The natural frequencies of these modes are 0.79 Hz and 0.97 Hz respectively, while the target frequencies calculated from the similarity law are 0.80 Hz and 0.98 Hz. The logarithmic decrements of these modes are 0.021 and 0.035 respectively. Therefore, the elastic model has sufficient accuracy for the elastic model tests. The displacement of the model is measured by laser displacement sensors (Keyence, IL-300, IL-600 and IL-2000). In order to obtain statistically stable data in low wind speeds in the wind tunnel, the measurement is carried out with a sampling frequency of 1.0 kHz and a data number of 393,216. This data length corresponds to 80 min. in real scale.

Experimental Results

Static Wind Force Coefficients

The mean drag, lift, and moment coefficients defined in the structural axis are evaluated in both smooth and turbulent flows. These coefficients are defined as follows;

$$Drag = \frac{1}{2} \rho U^2 B L C_D \quad (1)$$

$$Lift = \frac{1}{2} \rho U^2 B L C_L \quad (2)$$

$$Moment = \frac{1}{2} \rho U^2 B^2 L C_M \quad (3)$$

where *Drag*, *Lift*, and *Moment* are the mean wind forces, ρ is the air density, U is the mean wind speed, B is the deck width, L is the model length, and C_D , C_L , C_M are the drag, lift, and moment coefficients, respectively.

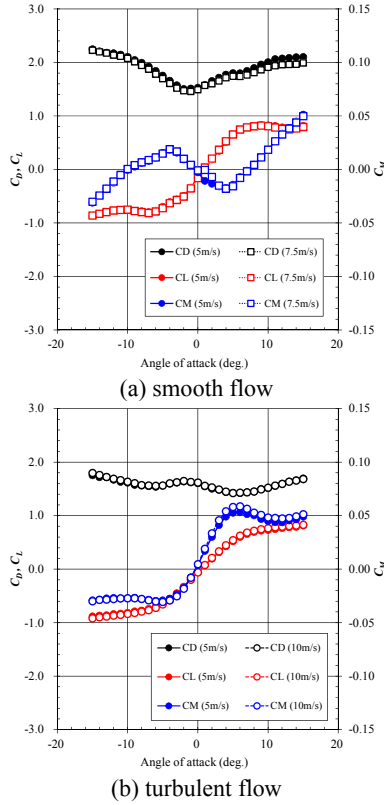


Figure 7. Mean wind force coefficients

The static wind force coefficients measured in smooth and turbulent flows are shown in Figure 7. The blockage ratio at the high angle of attack is more than 5%. Some results may have shown the effect of blockage; however, results at low angles of attack are not affected by blockage. All coefficients are only slightly affected by the Reynolds number effect. The gradients of lift force coefficients (lift gradients) are 10.24 and 7.88 in smooth flow and turbulent flow, respectively. The lift gradient of the thin plate is 2π , and the measured lift gradients are larger than that of the thin plate.

Aerodynamic Wind Force Coefficients

Unsteady aerodynamic wind forces acting on the model are measured in both smooth and turbulent flows, and they are evaluated using flutter derivatives defined by Scanlan & Tomko [5] as follows:

$$Lift = \rho b^2 \omega_F H_1^* \dot{\eta} + \rho b^3 \omega_F H_2^* \dot{\phi} + \rho b^3 \omega_F^2 H_3^* \phi + \rho b^2 \omega_F^2 H_4^* \eta \quad (4)$$

$$Moment = \rho b^3 \omega_F A_1^* \dot{\eta} + \rho b^4 \omega_F A_2^* \dot{\phi} + \rho b^4 \omega_F^2 A_3^* \phi + \rho b^3 \omega_F^2 A_4^* \eta \quad (5)$$

where H_1^* - H_4^* and A_1^* - A_4^* are flutter derivatives, b is the half deck width ($=B/2$), ω_F is the flutter circular frequency, η is the vertical displacement, and ϕ is the torsional displacement. The measured flutter derivatives in turbulent flow are shown in Figure 8. To investigate the flow characteristic effect on aerodynamic damping, H_1^* and A_2^* measured in smooth flow are also plotted in Figure 8. A_2^* in turbulent flow is almost 0 for all wind speeds, and it becomes positive at a certain wind speed in smooth flow. H_1^* has a negative value in both flows, and the absolute values of H_1^* in turbulent flow are lower than those in smooth flow. This result indicates that aerodynamic damping may be overestimated when H_1^* in smooth flow is used for damping evaluation.

Elastic Model Tests

The vertical amplitude at the end of the deck is measured in the free vibration tests using the elastic model. The maximum and

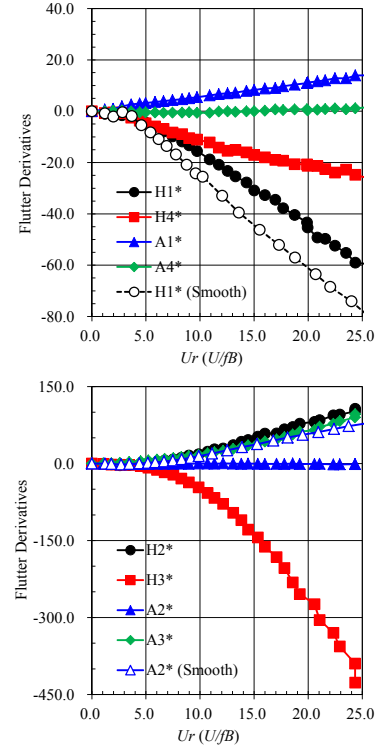


Figure 8. Flutter derivatives in turbulent flow

RMS amplitudes are evaluated from time histories at each wind speed, and the results are shown in Figure 9. The power spectrum density of the vertical oscillation at the end of the deck at the design wind speed is shown in Figure 10. The maximum vertical amplitude within the design wind speed is approximately 2.2 m. This maximum amplitude is generated mainly by the 1st vertical mode, as shown in Figure 10.

Gust Response Analysis

Analysis Theory and Conditions

Gust response analyses are conducted to compare the analysis results with the free vibration test results and to investigate the accuracy of the analysis. The method used in this study is that used in the wind resistant design for the Honshu-Shikoku bridges [3]. In the method, the cross-spectrum of the gust response of the bridge deck can be expressed using the matrix form as follows:

$$[S_{r_i, r_j}(\omega)] = [\phi] [0 \setminus |H_k(\omega)|^2 \setminus 0] [0 \setminus \{\phi_k\}^T [R u_{i_i} u_{j_j}(\omega)] \{\phi_k\} \setminus 0] [\phi]^T |H a_I(\omega)|^2 S u_I(\omega) \quad (6)$$

where $[S_{r_i, r_j}(\omega)]$ is the cross-spectrum of the response amplitude, i and j are the longitudinal positions on the bridge, ω is the circular frequency, $[\phi]$ is the modal matrix, $|H_k(\omega)|$ is the mechanical admittance of the k -th mode, $\{\phi_k\}$ is k -th modal vector, $[R u_{i_i} u_{j_j}(\omega)]$ is the spatial correlation matrix of the u_i component, $|H a_I(\omega)|$ is the aerodynamic admittance function, $S u_I(\omega)$ is the power spectrum of u_i component. The Busch & Panofsky spectrum [1] is used for obtaining the power spectrum of vertical fluctuating wind. The spatial correlation function and aerodynamic admittance can be expressed respectively as follows:

$$R u_{i_i} u_{j_j}(\omega) = \exp \left\{ \frac{-2}{\bar{U}_{i_i} + \bar{U}_{j_j}} \frac{\omega}{2\pi} \sqrt{(K_1 \Delta_x)^2 + (K_2 \Delta_y)^2} \right\} \quad (7)$$

$$|H a_I(\omega)|^2 = \left(\frac{\rho (dC_F / d\alpha) A_L \bar{U}_0^2}{2} \right)^2 |X_L^w(\omega)|^2 / \bar{U}_0^2 \quad (8)$$

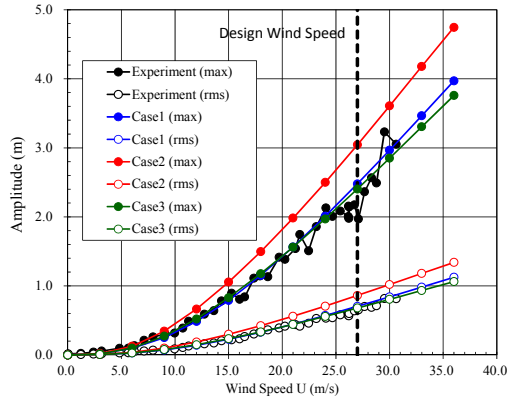


Figure 9. Max. and RMS gust response amplitudes (in real-scale)

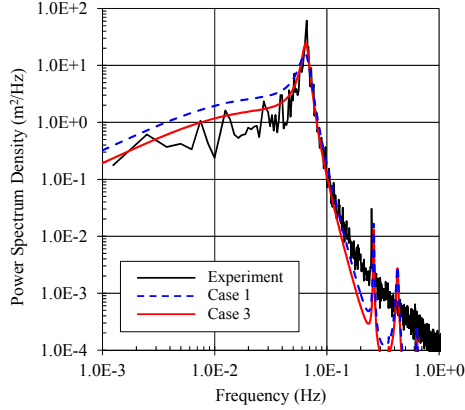


Figure 10. PSD of vertical oscillation (in real-scale)

	Deck (smo.)	Deck (turb.)	Tower
Lift Gradient	10.24	7.88	3.45
Tower Width	5.0m	Struct. Damp. (δ)	0.02
Power Index	0.12	Turb. Intensity	6.5%
Decay Factor	8.0	Evaluation Time	80min.

Table 2. Parameters used in gust response analysis

where \overline{U}_l is the mean wind speed of the l component at the i position, K_1 and K_2 are the decay factor in the longitudinal and vertical directions, Δ_x and Δ_y are the distance between the i and j positions. $dC_F/d\alpha$ is the lift gradient, A_{Li} ($= BL_i$) is the projected area of the i element, B is the deck width, L_i is the length of the i element, and \overline{U}_0 is the target wind speed.

$$|X_L^w(\omega)| = (a + \eta) / (a + (\pi a + 1)\eta + 2\pi\eta^2) \quad (9)$$

where $a = 0.1811$, $\eta = \omega B / 2\overline{U}_0$.

The evaluation of aerodynamic damping can be an important factor in gust response analysis. Two methods are used in this study. One is based on the quasi-steady theory, and the other is based on multi-mode flutter analysis. In the quasi-steady method, the aerodynamic damping can be expressed as follows:

$$\zeta_{ak} = \{\phi_k^D\}^T \left[0 \setminus \frac{\rho(dC_F/d\alpha)A_{Li}\overline{U}_0}{4\omega_k} \setminus 0 \right] \{\phi_k^D\} \quad (10)$$

where $\{\phi_k^D\}$ is the vertical component vector of deck k -th mode. In the multi-mode flutter analysis method, the result that uses measured flutter derivatives in turbulent flow is used for the evaluation of aerodynamic damping.

The effect of wind force acting on the tower is also included in the evaluation of the gust response using a method similar to the method for decks. The contribution of the wind force acting on the tower on the amplitude is less than 10% at the design wind speed. Table 2 lists other parameters used in the gust response analysis. Gust response analyses were conducted for three cases as shown in Table 3. The quasi-steady theory and results of

Case name	Aerodynamic damping	Lift gradient
Case 1	Quasi-steady theory	Smooth flow
Case 2	Multi-mode flutter analysis	Smooth flow
Case 3	Multi-mode flutter analysis	Turbulent flow

Table 3. Analysis cases of gust response analysis

multi-mode flutter analyses are used to evaluate aerodynamic damping. Lift gradients in smooth flow or in turbulent flow are used to evaluate the aerodynamic admittance in Equation (8).

Results of Gust Response Analyses

The results of gust response analyses are plotted in Figure 9. The maximum amplitude and RMS amplitude of Case 1 are in good agreement with the experimental result in all velocity ranges. However, the power spectrum of the vertical oscillation at the end of the deck plotted in Figure 10 has an apparent discrepancy in the shape around the 1st mode natural frequency. As shown in Figure 8, the aerodynamic damping in the vertical direction in turbulent flow is much lower than that in smooth flow. In quasi-steady theory, the lift gradient in smooth flow is used, and it may have overestimated the aerodynamic damping. The overestimation of damping causes the difference in the power spectrum density. The lift gradient in smooth flow leads to overestimation of the aerodynamic admittance. As a result of these two overestimations, the estimated amplitude appears to coincide with the experimental result. The results of Case 2 overestimate the amplitude in all velocity ranges. The aerodynamic admittance is still overestimated in Case 2, while aerodynamic damping is evaluated properly using multi-mode flutter analysis results. The results of Case 3 are in good agreement with the experimental results in all velocity range. The power spectrum density also agrees well with experimental result. Both aerodynamic damping and aerodynamic admittance are evaluated properly in Case 3. It was clarified that the vertical gust response amplitude of long-span cable-stayed bridges under erection could be evaluated appropriately by gust response analysis when appropriate wind force coefficients are used.

Conclusions

The following conclusions were derived through this study.

- The result of the vertical gust response analysis of a cable-stayed bridge under erection is in good agreement with the result of the elastic model test when appropriate wind force coefficients are used.
- Aerodynamic damping from multi-mode flutter analysis and aerodynamic admittance evaluated from the lift gradient in turbulent flow enables appropriate gust response evaluation.
- Aerodynamic damping is overestimated in quasi-steady theory, and aerodynamic admittance appears to be overestimated when the lift gradient in smooth flow is used. However, these two overestimations led to the results of the gust response analysis being in good agreement with the experimental results.

Future research will be conducted with the aim of investigating the effect of wind direction on gust response evaluation. The accurate evaluation of gust response for any wind direction is needed for wind-resistant design of long-span bridges under erection.

References

- [1] Busch, N.E., Panofsky, H.A., *Recent spectra of atmospheric turbulence*, Q.J. Roy. Meteor. Soc., vol.94, pp. 132-148, 1968. [2] ESDU74031, Characteristics of atmospheric turbulence near the ground part III, 1974. [3] Honshu-Shikoku Bridge Authority, *Wind Proof Design Standard for Honshu-Shikoku Bridges*, 2011. [4] Kimura, K., Tanaka, H., Bridge buffeting due to wind with yaw angles, J. of Wind Eng. and Ind. Aerody., pp. 1309-1320, 1992. [5] Scanlan, R.H., Tomko, J.J., Airfoil and bridge deck flutter derivatives, J. of the Engineering Mech. Div., 1971.